

1 **Interaction between East Asian summer monsoon and westlies as**
2 **shown by tree-ring records**

3

4 Xiao Shengchun^{1*}, Peng Xiaomei¹, Tian Quanyan¹, Ding Aijun², Xie Jiali¹, Su
5 Jingrong^{1,3}

6

7 ¹ Key Laboratory of Ecological Safety and Sustainable Development in Arid Lands,
8 Northwest Institute of Eco-Environment and Resources, Chinese Academy of
9 Sciences, Lanzhou, Gansu, China 730000.

10 ² College of Resources and Environment, Gansu Agricultural University, Lanzhou,
11 Gansu, China 730070.

12 ³ University of Chinese Academy of Sciences, Beijing, China 100049.

13 * Corresponding author (xiaosc@lzb.ac.cn).

14 Address: 320 West Donggang Road, Lanzhou City, Gansu Province, China.

15 Zip Code: 730000.

16

17 **Abstract:**

18 Atmospheric circulation changes, their driving mechanisms and interactions are
19 important topics in global change research. Local changes in the East Asian summer
20 monsoon (EASM) and the mid-latitude westlies will inevitably affect the climate and
21 ecology of the arid zone of Northwest China. Hence, it is important to study these
22 regional changes. While previous studies in this area are all single-point climate
23 reconstruction studies, there is a lack of research on the interaction areas and driving
24 mechanisms of the two major circulations. Dendroclimatology can provide high-
25 resolution, long-term, and reliable multi-point proxies for the study of inter-annual and
26 inter-decadal climate change. We chose to observe these changes in the Alxa Plateau
27 using dendrochronological methods. We assembled ring-width records of Qinghai
28 spruce (*Picea crassifolia*) in the mountain regions surrounding the Alxa Plateau: the
29 Helan Mountains, Changling Mountain, and Dongdashan Mountain. The results show
30 that radial growth was indeed affected by changes in the monsoon and westerlies. The
31 heterogeneity of precipitation and climatic wet-dry changes in different regions is
32 primarily influenced by the interactions between atmospheric circulation systems, each
33 with its own dominant controlling factors. In the case of the Helan Mountains, both of
34 these major atmospheric circulation systems play a significant role in shaping climate
35 changes. Changling Mountain in the southern part of the Alxa Plateau is mainly
36 influenced by the EASM. Dongdashan Mountain is mainly influenced by the westerlies.
37 Understanding these local conditions will help us predict climate changes in Northwest
38 China.

39

40 **Key words:** Alxa Plateau, dendroclimatology, westerlies, EASM, interaction between
41 winds and monsoon.

42

43 **1. Introduction**

44 The alpine zone of Qinghai-Tibet, the arid zone of the northwestern interior, and
45 the humid zone of the east constitute the three main areas of China's natural
46 geomorphology (Chen et al., 2019a). The Northwest China inland dry zone is located
47 in the hinterland of the Eurasian continent and is among the driest regions in the world.
48 It displays typical climatic characteristics of a continental climate. This region is mainly
49 influenced by westlies and the EASM (the East Asian summer monsoon). The
50 interaction of these two factors results in high precipitation variability and hence
51 frequent droughts. This was true even before the onset of global climate change in the
52 area, and it is even more pronounced in recent years. This inland arid zone is
53 ecologically fragile (Chen et al., 2019a; Chen et al., 2019b; Zhang et al., 2023).

54 The semi-arid and arid regions of northern China are characterized by large areas
55 of sand and desert. They are the second largest source of dust in the world after the
56 Sahara. Their contribution to global climate change is large. So far inland, the influence
57 of the EASM is often weak (Zhang et al., 2021; Liu et al., 2022). It is opposed by the
58 westerlies that flow from the North Atlantic climate zone toward the East Asian
59 monsoon climate zone (Qu et al., 2004). The interaction between the westerlies and the
60 EASM governs precipitation, water vapor transport, and thus the climate of
61 northwestern China (Feng et al., 2004; Wang et al., 2005; Li et al., 2008; Ma et al.,
62 2011).

63 To estimate the impact of global change on this interaction, it is crucial to
64 comprehend its historical context. Global atmospheric circulation is likely to change,
65 as is the EASM. Climate change will not only affect the regional climate and regional
66 water resources (Ding et al., 2023); it will affect East Asia (dust storms) and even the
67 rest of the globe. Hence, the study of climate in this region is of great practical and
68 theoretical significance (Chen et al., 2019a; Chen et al., 2019b).

69 The westerlies and the EASM meet at the northern boundary of the Asian summer
70 monsoon (Huang et al., 2023). In northern China, this boundary runs from west to east,
71 along the eastern section of the Qilian Mountains, the southern foothills of the Helan
72 Mountains, the Daqing Mountains, and the western section of the Daxinganling

73 Mountains. This is not a static boundary. It fluctuates within a range of 200–700 km
74 (Chen et al., 2018). It is important to understand the history of these fluctuations (Huang
75 et al., 2023).

76 This can be done using climate records such as lacustrine, eolian, and
77 dendrochronological (Sun et al., 2003; Liu et al., 2005; Li, 2009; Chen et al., 2010; Li
78 et al., 2016; Chen et al., 2019b; Qin et al., 2023). Dendrochronology is one of the best
79 tools for studying paleoclimatic changes, due to its precise dating, high resolution, good
80 continuity and high replication (Zhang et al., 2003; Shao et al., 2010; Yang et al., 2014;
81 Liu et al., 2016).

82 The climate history of the Baotou area, at the northern edge of the EASM, has been
83 studied at interannual and interdecadal scales for the past 260 years, based on June–
84 August precipitation reconstruction from tree-ring samples from the western Yinshan
85 Mountains (Liu et al., 2001; Liu et al., 2003). Using tree-rings and historical records,
86 Kang and Yang (2015) reconstructed the annual precipitation history of the East Asian
87 monsoon northern fringe zone for the last 530 years. They analyzed spatial variability
88 and possible driving mechanisms using the 400-mm isohyet.

89 Several May–July precipitation sequences have been reconstructed using ring-
90 width and latewood-width data from Chinese pine (*Pinus tabulaeformis*) growing in
91 the Helan Mountains (Ma et al., 2003; Liu et al., 2004; Chen et al., 2016). Studies of
92 tree-ring carbon and oxygen isotopes from Chinese pine samples have shown that $\delta^{18}\text{O}$
93 values increase with summer precipitation, while $\delta^{13}\text{C}$ values decrease (Zhang et al.,
94 2005a; Liu et al., 2008). westerlies have also been shown to affect precipitation in the
95 Helan Mountains (Chen et al., 2010).

96 Principal component analysis of tree-ring chronologies constructed from data
97 collected at several sites in Gansu suggests that trees at these sites were more influenced
98 by EASM than by westerlies (Chen et al., 2013). These researchers also found that the
99 EASM weakened in 1970s, but recovered in the early 1990s. Tree-ring data allowed the
100 reconstruction of 330 years of PDSI (Palmer Drought Severity Index) values for the
101 Mount Hasi region (at the northern boundary of the summer monsoon zone) (Kang et
102 al., 2012). This study confirmed that radial growth of Chinese pine has declined over

103 the past three decades, due to the weakening of the EASM. Dendrochronological
104 reconstruction of precipitation in the Mount Changling region (again using Chinese
105 pine) suggested that precipitation in that region mainly depends on the EASM (Chen et
106 al. 2012). Other researchers have assembled tree-ring chronologies from pines growing
107 in the Mount Qilian region and the northern mountains of the Hexi Corridor. Here again
108 precipitation is associated with the EASM. These chronologies have allowed scholars
109 to compile precipitation, temperature, and drought records for the last thousand years
110 (Gou et al., 2015a; Gou et al., 2015b; Zhang et al., 2017).

111 Most modern researchers studying climate change in the region are mostly carried
112 out on single sample sites (Wang et al., 2004; Liu et al., 2005; Chen et al., 2010; Chen
113 et al., 2016; Li et al., 2016; Liu et al., 2016; Chen et al., 2018). While, there is a dearth
114 of multi-site, regional and long time scale studies on the interaction of the westerlies
115 and the EASM. The research focuses on the interplay area, and investigates the
116 spatiotemporal heterogeneity in climate change and its dominant driving factors,
117 specifically related to the westerlies and East Asia monsoon circulation in Alxa Plateau.

118 Compiled and analyzed tree-ring chronologies from Qinghai spruce (*Picea*
119 *crassifolia*) growing in the Helan, Changling, and Dongdashan mountain regions that
120 surround the Alxa Plateau, the climate response characteristics of spruce radial growth
121 in three regions was then analyzed. Combining the relevant Westerly and East Asia
122 monsoon circulation indices, the driving mechanism of the regional climate change by
123 with the interaction and synergistic roles of two atmospheric circulation systems in the
124 Alxa Plateau was explored. The results will lay a theoretical foundation for the climatic
125 evolution of the region and the desertification control.

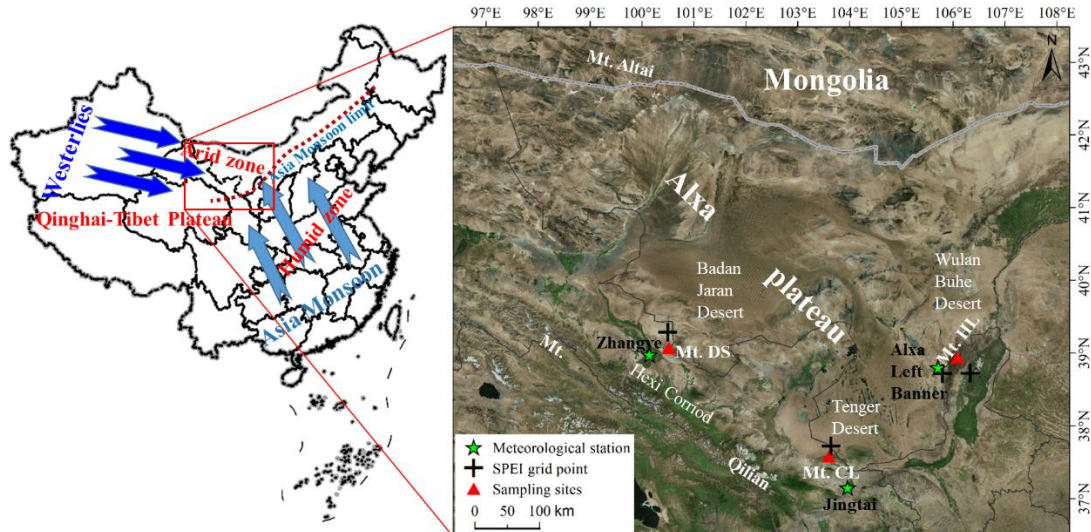
126

127 **2. Material and methods**

128 **2.1 Study area**

129 The Alxa Plateau is located in the western part of the Inner Mongolia Autonomous
130 Region and is surrounded by mountains (Fig.1). It consists primarily of three deserts:
131 Tengger, Ulan Buh, and Badan Jaran. It lies south of the Gobi desert. It is the main
132 source of the fierce sandstorms and dust storms that blow toward eastern China and the

133 Pacific. It has been much affected by climate change; sand- and dust storms have
 134 increased, much to the detriment of lands to the east. The Chinese government is doing
 135 what it can to establish an environmental defense line there. It is currently the Northern
 136 Sand Prevention Belt of the National Two Ecological Barrier and Three Belts
 137 Ecological Security Strategy Pattern (Xiao et al., 2017; Xiao et al., 2019).



138
 139 Figure 1. Location of tree-ring sampling sites and meteorological stations (the right
 140 panel is from Mapworld).
 141

142 There are several mountain ranges surrounding the Alxa Desert, such as the Helan
 143 Mountains in the east, the northern mountains of the Hexi Corridor, and the outliers of
 144 the Altai Mountains in the north. These mountains not only block the eastward and
 145 southward expansion of the desert (driven by high pressure regions from Mongolia);
 146 they are also the source of mountain rivers and streams that water the oases on the
 147 plateau.

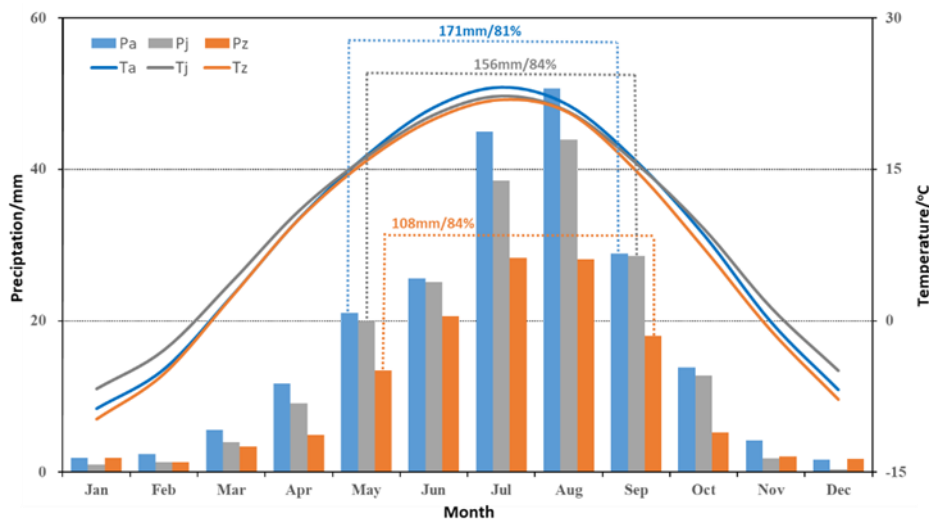
148 The Alxa Plateau is located in the eastern margin of the inland arid region of Central
 149 Asia. It is affected not only by the mid-latitude westerly circulation, but also by the
 150 Asian monsoon and the plateau monsoon. It is in the zone where the mid-latitude
 151 westerly circulation and the Asian monsoon interact (Xiao et al., 2017; Chen et al.,
 152 2019b). As a result, there is large interannual variability of vegetation cover in the
 153 region (Ou and Qian, 2006; Tang et al., 2006; Li et al., 2013).

154 The Helan Mountains (38°27'~ 39°30'N, 105°20'~106°41'E) (sampling site
 155 henceforth abbreviated as HL), are located at the eastern edge of the Tengger Desert.
 156 They stretch more than 200 kilometers from north to south; the main peak is ~3,556 m.
 157 The mountain forests are dominated by Qinghai spruce and Chinese pine, juniper,
 158 mountain aspen, and elm.

159 Mount Changling (37°12'~37°17', 102°45'~103°48'E) (sampling site henceforth
 160 abbreviated as CL) is an independent mountain protruding northward from the
 161 remnants of the eastern Qilian Mountains, it is located at the southern edge of the
 162 Tengger Desert; its elevations range from 2100 to 2900 m. The dominant tree species
 163 are Qinghai spruce and Chinese pine.

164 Mount Dongdashan (39°00'~39°04'N, 100°45'~100°51'E) (sampling site
 165 henceforth abbreviated as DS) is located at the southwestern edge of the Badan Jaran
 166 Desert and the middle part of Mount Qilian. It is one of the northern mountains along
 167 the Hexi Corridor; that range consists of mountains that vary from 2200 to 2637 m in
 168 elevation. Forests are dominated by Qinghai spruce and Qilian juniper.

169 The temperatures of the coldest months recorded at meteorological stations in the
 170 Alxa Left Banner (a division of the Alxa League region), Jingtai (a county in Gansu),
 171 and Zhangye (a city in Gansu) all occurred in January, ranging from -9.8°C to -6.8°C.
 172 The hottest months at those stations were in July (21.9 °C to 23.1 °C). These
 173 meteorological stations are the closest stations to our three sampling sites.



174

175 Figure 2. Climatic diagram of study area. Pa/Ta are the monthly total precipitation and
176 monthly mean temperature at the Alxa Left Banner meteorological station (1953–2016);
177 Pj/Tj are the precipitation and temperature figures for the Jingtai meteorological station
178 (1957–2017); Pz/Tz are the precipitation and temperature figures for the Zhangye
179 meteorological station (1957–2017). The dashed box and appended data indicate the
180 total growing season precipitation in the study area and the proportion of total annual
181 precipitation.

182 Precipitation measured at those stations varied widely. The multi-year average of
183 total precipitation from May to September was 171 mm at Alxa Left Banner station,
184 156 mm at Jingtai station, and 108 mm at Zhangye station. This accounted for more
185 than 80% of the annual precipitation (Fig.2).

186

187 **2.2 Sample collection, processing and data analysis method**

188 **2.2.1 Sample collection, processing and dendrochronology construction**

189 Researchers used standard methods of tree-ring sample collection. One core was drilled
190 from each tree in the sample site. We collected 209 cores in total, from five sampling
191 sites at HL, 48 cores from one sampling site at CL, and 81 cores from two sampling
192 sites at DS. Relevant information of the sampling sites is summarized in Table 1.

193 Chronologies were constructed using standard dendrochronological methods
194 (Cook, 1985). In order to highlight the high frequency signal, the RES chronology is
195 selected for later climate analysis. We calculated the highly significant correlations (P
196 < 0.001) between the chronologies of different points at the HL and DS mountains; a
197 weighting method was used to finally synthesize a chronology for each mountain.
198 Generally, the sub-sample signal strength (SSS) index and the mean series
199 intercorrelation (R_{bar}) are used to evaluate the credibility and quality of the chronologies.
200 The length of the reliable chronology is indicated by the parts of the series with a
201 subsample signal strength (SSS) index > 0.85 (Wigley et al., 1984). Another important
202 statistic is the mean series intercorrelation (R_{bar}), which is the mean correlation
203 coefficient among the ring series and is therefore an indication of the common variance.

204

205 **2.2.2 Climate data, atmospheric circulation indices and the related Analyzing**
206 **methods for chronological correlation**

207 Climate data for the study areas HL, CL, and DS were collected from the nearest
208 meteorological stations in Alxa Left Banner, Jingtai and Zhangye, respectively
209 (<http://data.cma.cn>).

210 We used SPEI (Standardized Precipitation Evapotranspiration Index) to represent
211 the local drought and wetness conditions, which is widely used in the dendrochronology
212 studies and considering the effects of potential evapotranspiration, precipitation and
213 time scales (Vicente-Serrano et al., 2010). SPEI data (grid-point resolution $0.5^{\circ} \times 0.5^{\circ}$)
214 was obtained from the grid-point datasets of the National Center for Environmental
215 Predictions-National Center for Atmospheric Research (NCEP-NCAR). Time scales
216 ranged from 1 month to 15 months. The mean values of data from two grid-points
217 closest to the HL sampling site (38.75°N , 105.75°E and 38.75°N , 106.25°E ; period
218 1953–2015) were chosen for subsequent analysis. Grid-point data from one site closest
219 to our CL sampling site (37.75°N , 103.75°E ; period 1951–2015) was used for later
220 analysis. Grid-point data from one site closest to our DS sampling site (39.25°N ,
221 100.75°E ; period 1951–2015) was also used. As SPEI datasets are multi-scale, we
222 preprocessed the data to identify and select 11-month scaled SPEI datasets for
223 subsequent analysis.

224 We took into account the so-called lagging effect (the influence of fall and winter
225 climate factors on the radial growth of trees shows up later in the year) and chose to use
226 temperature, precipitation, and SPEI data from September of the previous year to
227 September of the current year (abbreviated as P9–P12 and C1–C9), as collected at each
228 meteorological station, for our climate response analysis.

229 The East Asian Summer Monsoon Index (EASMI) (Li and Zeng 2005) represents
230 the activity strength of the EASM. Larger EASMI values indicate a stronger summer
231 monsoon, smaller ones a weaker monsoon. In this study, the EASMI (mean values for
232 June–August in the period 1950–2017) defined by Li and Zeng (2005) was used to
233 study the impact of the EASM on climate change in the study area.

234 The East Asian Summer Monsoon Index (EASMI) represents the activity strength
235 of the EASM. The East Asian summer monsoon (EASM) index is defined as an area-
236 averaged seasonally (JJA) dynamical normalized seasonality (DNS) at 850 hPa within
237 the East Asian monsoon domain (10°-40°N, 110°-140°E) (Li and Zeng 2005). Larger
238 EASMI values indicate a stronger summer monsoon, smaller ones a weaker monsoon.
239 In this study, the EASMI (mean values for June–August in the period 1950–2017)
240 defined by Li and Zeng (2005) was used to study the impact of the EASM on climate
241 change in the study area.

242 We used the Westerly Circulation Index (WCI annual mean; [https://cmdp.ncc-](https://cmdp.ncc-cma.net/cn/index.htm)
243 [cma.net/cn/index.htm](https://cmdp.ncc-cma.net/cn/index.htm)) to represent the strength of the mid-latitude westerlies. The
244 larger the WCI value, the stronger the Eurasian latitudinal circulation; the smaller the
245 value, the weaker the Eurasian latitudinal circulation. WCI data (period 1951–2015)
246 were derived from the Eurasian Latitudinal Circulation Index published by the National
247 Climate Center of the China Meteorological Administration ([https://cmdp.ncc-](https://cmdp.ncc-cma.net/cn/index.htm)
248 [cma.net/cn/index.htm](https://cmdp.ncc-cma.net/cn/index.htm)).

249 Interannual and interdecadal (sliding moving average of 11a) chrono-climatic/-
250 cyclonic index correlation and partial correlation analyses were performed using SPSS
251 19.0. Based on the characteristics of tree-ring series, the sequences were classified into
252 three groups of low, average and high ring widths using mean $\pm 1\delta$ (δ : standard
253 deviation) as the classification criterion (with mean $\pm 2\delta$ as the extreme year).
254 Correlation statistical tests were performed with the corresponding annual circulation
255 indices; similar treatments and analyses were performed for the two major circulation
256 indices.

257

258 **3. Results and analysis**

259 **3.1 Ring-width chronologies and their characteristics**

260 Based on the sampling cores from five sample sites at HL, two sample sites at DS, and
261 one sample site at CL, ring-width residual chronologies were derived for each of the

262 three study areas (Fig. 3). Statistical parameters showed that the three chronologies
 263 meet the usual requirements for correctly done dendrochronological studies (Table 1).

264 Table 1. Statistical characteristics of the sampling sites and the tree-ring chronologies.

265

266 Table 1. Statistical characteristics of the sampling sites and the tree-ring chronologies.

Sampling sites	HL(5)	CL(1)	DS(2)
Latitude (°N)	38.52–38.97	37.61	39.04
Longitude (°E)	105.83–106.02	103.71	100.78
Elevation (m)	2200–2750	2490	2650–2700
Cores	209	48	81
Reliable period	1891–2018	1866–2017	1823–2015
MS	0.18–0.37	0.28	0.15–0.33
R_{bar}	0.45–0.61	0.56	0.40–0.60
SNR	22.5–56.1	38.9	25.7–42.5
EPS	0.96–0.98	0.98	0.96–0.98
PC1(%)	17.3–63.0	57.9	43.0–62.5

267 Reliable period (SSS > 0.85), MS (mean sensitivity), R_{bar} (mean series intercorrelation), SNR (signal to
 268 noise ratio), EPS (expressed population signal), and PC1 (variance explained by the first principal
 269 component) refer to residual chronologies).

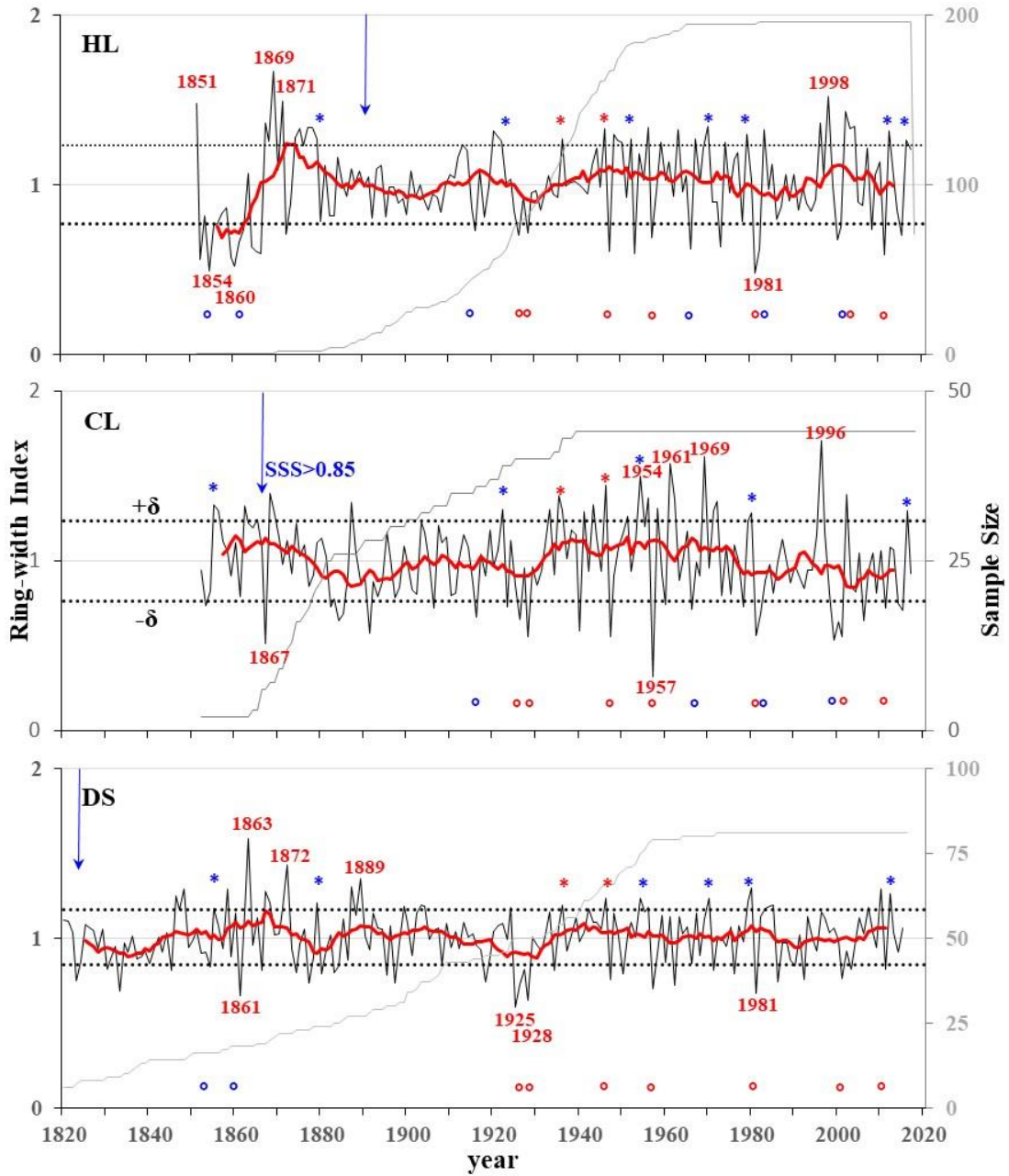
270

271 3.2 Climate response characteristics

272 Correlation analysis comparing a) monthly mean temperature and precipitation at
 273 neighboring meteorological stations and b) SPEI at the nearest grid-point showed that,
 274 overall, the three residual chronologies were correlated negatively with monthly mean
 275 air temperature, positively correlated with monthly precipitation, and positively
 276 correlated with SPEI during the growing season (Fig. 4).

277 HL chronology was correlated negatively with mean temperature mainly in C5–C8
 278 in the growing season, but not to the significant level. It was also positively correlated
 279 with precipitation in all months except P12, C1, and C9, reaching significant levels (P
 280 < 0.05) in P9, C5, and C6. All months were positively correlated with SPEI and reached

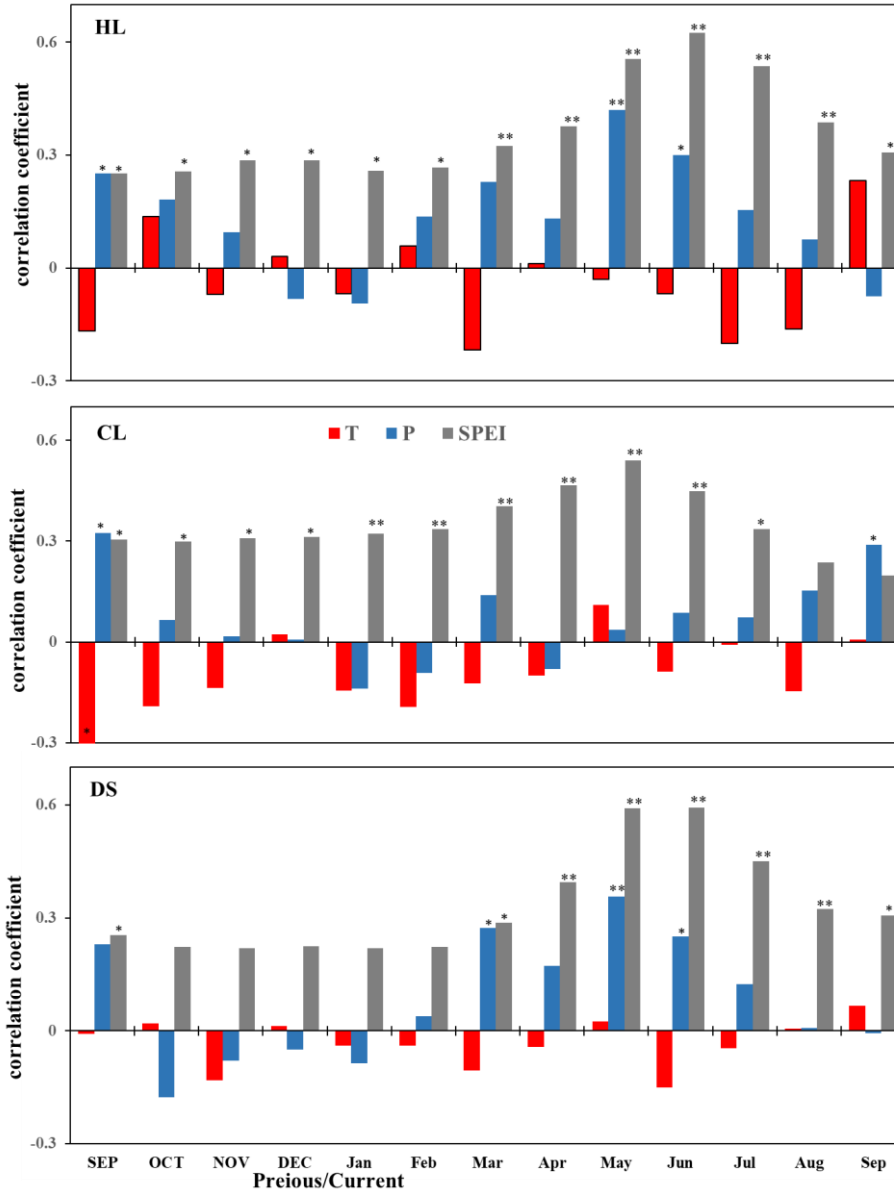
281 statistical significance ($P < 0.05$), with C3–C8 showing highly significant correlation
 282 levels ($P < 0.01$).
 283



284
 285 Figure 3. Residual ring-width chronologies for the three study areas. The dark lines
 286 indicate the chronology; grey lines indicate the sample depth; red lines indicate the 11-
 287 year running mean chronology; dotted horizontal lines indicate the mean value $\pm 1\delta$;
 288 years with data identified as $>/< \text{mean} \pm 2\delta$ (δ : standard deviation); blue * and o indicate
 289 the years shared between two of the three sample sites, red * and o shows years shared

290 between three sample sites; blue arrows indicate the start of the reliable residual
 291 chronology ($SSS > 0.85$).

292



293

294 Figure 4. Correlation coefficients (Pearson's r values) between the residual ring-width chronologies
 295 of Qinghai spruce at the three study areas (HL, CL and DS) and the observed monthly temperature
 296 (T), total monthly precipitation (P), and SPEI. * Pearson's r correlation, significant at $P < 0.05$. **
 297 Pearson's r correlation, significant at $P < 0.01$. Month names of previous year are capitalized.

298 CL chronology was negatively correlated with the mean temperature in most
 299 months, but only reached a significant negative correlation ($P < 0.05$) with P9. CL
 300 chronology was positively correlated with monthly precipitation, save for C1, C2, and

301 C4. Only P9 and C9 reached statistical significance ($P < 0.05$). All months were
302 positively correlated with SPEI, with P9–C7 reaching significant correlation levels (P
303 < 0.05) and C1–C7 reaching highly significant correlation levels ($P < 0.01$).

304 DS chronology showed weak correlations between DS chronology and monthly
305 mean temperatures. None of the correlations reached levels of significance. DS
306 chronology was positively correlated with P9 and C2–C8 precipitation and reached
307 significant correlation levels for C3, C5, and C6 ($P < 0.05$). All months were positively
308 correlated with SPEI, with P9 and C3–C9 reaching significant correlation levels ($P <$
309 0.05) and C4–C8 reaching highly significant correlation levels ($P < 0.01$).

310 Overall, the radial growth of Qinghai spruce at the three study areas seems to have
311 been limited, for the most part, by low precipitation during the growing season (April–
312 July). The three chronologies reflect regional wet and dry variations.

313

314 **3.3 Regional climate changes as recorded by tree-ring widths**

315 **3.3.1 Regional climate change viewed at interannual scales**

316 On interannual scales, the three residual chronologies, when compare, showed highly
317 significant correlations (HL–CL: $n = 166$, $r = 0.298$, $P < 0.001$; HL–DS: $n=165$, $r=0.331$,
318 $P < 0.001$; CL–DS: $n = 164$, $r = 0.374$, $P < 0.001$). This indicates that there was a high
319 degree of consistency in the radial growth of Qinghai spruce in the three regions.

320 According to the results of the chronology-climate response analysis in the
321 previous section, the high and low ring-width indices ($\text{mean} \pm 1\sim 2\delta$) of the chronology
322 at the three sample sites indicate wetter or drier, and extreme wet or dry years,
323 respectively (Fig. 3).

324 Overall, the three ring-width residual chronologies (HL, CL, DS) had a total of two
325 shared wetter years and seven shared drier years. The HL and CL chronologies shared
326 four wet years and eleven dry years; the HL and DS chronologies shared five wet years
327 and nine dry years; and the CL and DS chronologies shared five wet years and seven
328 dry years (Fig. 3).

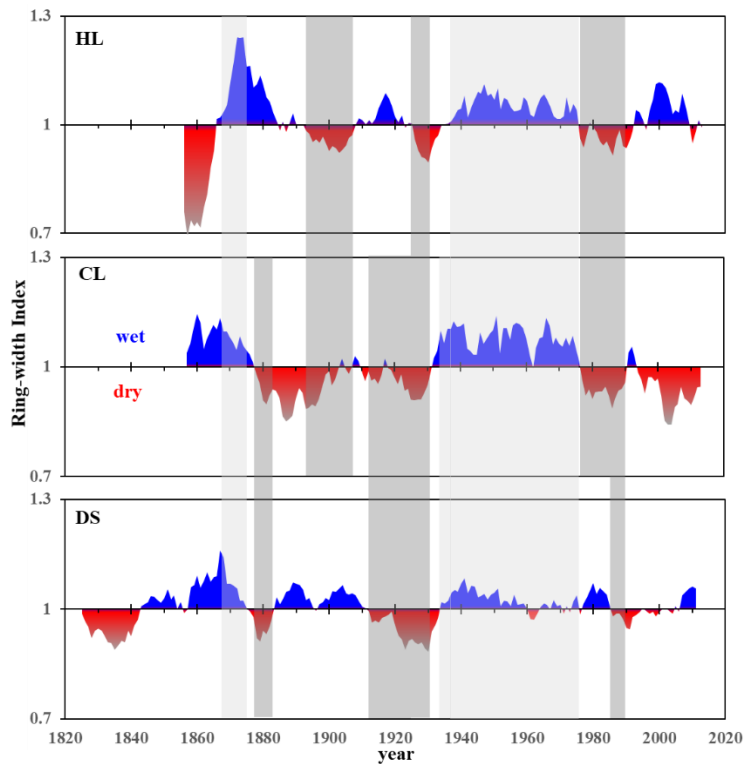
329 There were no extremely wet years shared by the three sample sites. However, there
330 were two shared wetter years in 1936 and 1946 and several shared wetter years in later
331 years among the three sample sites. For example, note the wetter years in 1922 and
332 2016 for HL and DS chronologies; 1959, 1979, and 2012 for HL and DS chronologies;
333 1855, 1954, and 1980 for CL and DS chronologies (Fig. 3).

334 The extreme drought years are consistent among the three sample sites. For
335 instance, there was an extreme drought year in 1981 at HL and DS sample sites; it was
336 also a drought year at CL. An extreme drought year at CL in 1957 was also a drought
337 year for the other two chronologies. Moreover, the extreme drought year of 1928 at DS
338 was a drought year at the other two sites. Drought years in 1926, 1947, 2001, and 2011
339 were seen in all three sites and in two of the three sample sites (1916, 1966, 1982, and
340 2000 at HL and CL; 1854 and 1861 at HL and DS) (Fig. 3).

341

342 **3.3.2 Characteristics of regional climate change at inter-decadal scales**

343 On the decadal scale, the 11a running mean series indicates that at the HL site there
344 were four wetter periods (mid-1860s to early 1880s; 1910s to 1920s; mid-1930s to mid-
345 1970s; and late 1990s to early 2010s). Four drought periods were seen (mid-1850s to
346 mid-1860s; early 1890s to late 1900s; circa 1930s; and mid-1970s to 1980s) (Fig.5).



347

348 Figure 5. Three regional chronologies demonstrating alternation between dry (red) and
 349 wet (blue) years on interdecadal scales (11 a running mean). The gray and light gray
 350 bands indicate consistent changes of the dry and wet periods.

351 The CL regional chronology revealed two main wetter periods (mid-1850s to mid-
 352 1870s; mid-1930s to mid-1970s) and two longer drought periods (late 1870s to early
 353 1930s; following the late 1970s) (Fig.5).

354 The DS regional chronology showed four main wetter periods (mid-1840s to mid-
 355 1870s; mid-1880s to late 1900s; mid-1930s to mid-1980s; and late 2000s to early
 356 2010s). There were four drought periods (mid-1820s to mid-1840s; mid-1870s to 1880s;
 357 early 1910s to early 1930s; and late 1980s to mid-2000s). The drought during the last
 358 drought period was less severe (Fig.5).

359 The three chronologies show both synchronized phases and differential changes on
 360 an interdecadal scale. The more synchronized dry phases of climate change were the
 361 drought periods of the 1930s and 1990s. When we compared the DS chronology to the
 362 HL and CL chronologies on decadal scales, we noted that DS droughts tended to last
 363 longer and that they started and ended later than CL droughts. However, HL and DS
 364 droughts tended to end at the same time (Fig.5).

365 There were two wet periods in 1870s and the mid-1930s to 1970s which were
366 shared by all three sample sites. The latter period was the longest lasting wet period we
367 saw in our study. There were also dry and wet periods that were not shared by any of
368 our sites. There was an HL drought (mid-1850s to mid-1860s) which was not shared by
369 the other two sites, which were wetter. HL and CL shared drought periods (1890s to
370 1910s; 1980s) while DS was wetter. Conversely wetter periods at HL were sometimes
371 accompanied by drought in the other two sites. Drought at CL was sometimes
372 accompanied by wet periods at the other two sites. DS was wet during the 2010s but
373 the other two sites were in drought (Fig.5).

374 The results of the above studies show that there are diversified and complex
375 features in the interdecadal processes of climate change in different regions around the
376 Alxa Plateau.

377

378 **3.4 Driving mechanism of the regional climate changes**

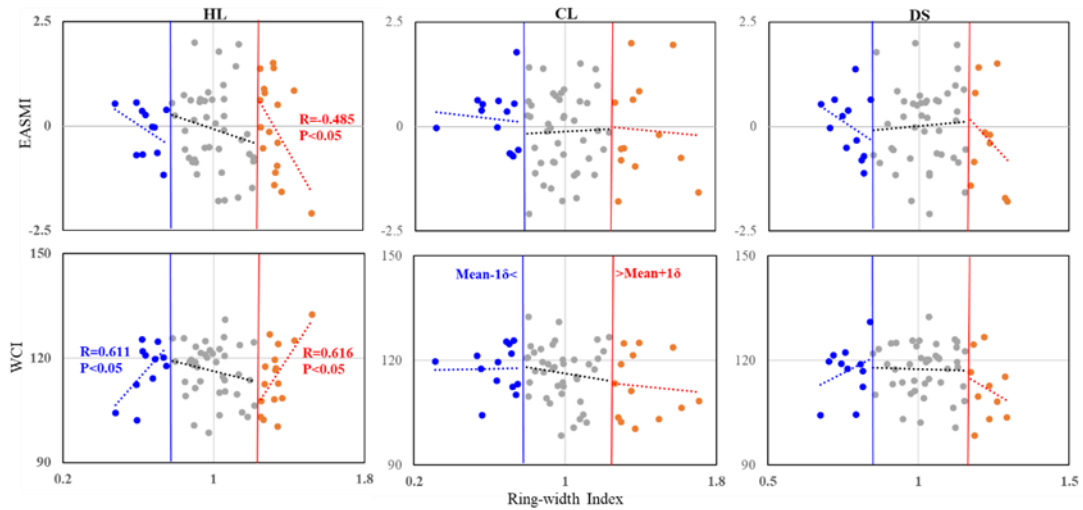
379 **3.4.1 Driving mechanism of the regional climate changes of typical years**

380 On the interannual scales, three regional chronologies we developed showed fairly
381 weak negative correlations between the EASM and the westerlies; none of the
382 correlations were statistically significant. We carried out correlation analyses of the
383 three regional ring-width chronologies and two major circulation indices. This was
384 done in high, medium and low ring-width index groups (Fig. 6; 7).

385 At HL, the results of our combined subgroup correlation analyses suggest that
386 correlations between radial growth groups and atmospheric circulations were stable.
387 Correlation between the higher ring-width group and atmosphere circulation indices
388 and between the lower ring-width group and the WCI were all significant ($P < 0.05$)
389 (Fig. 6; 7).

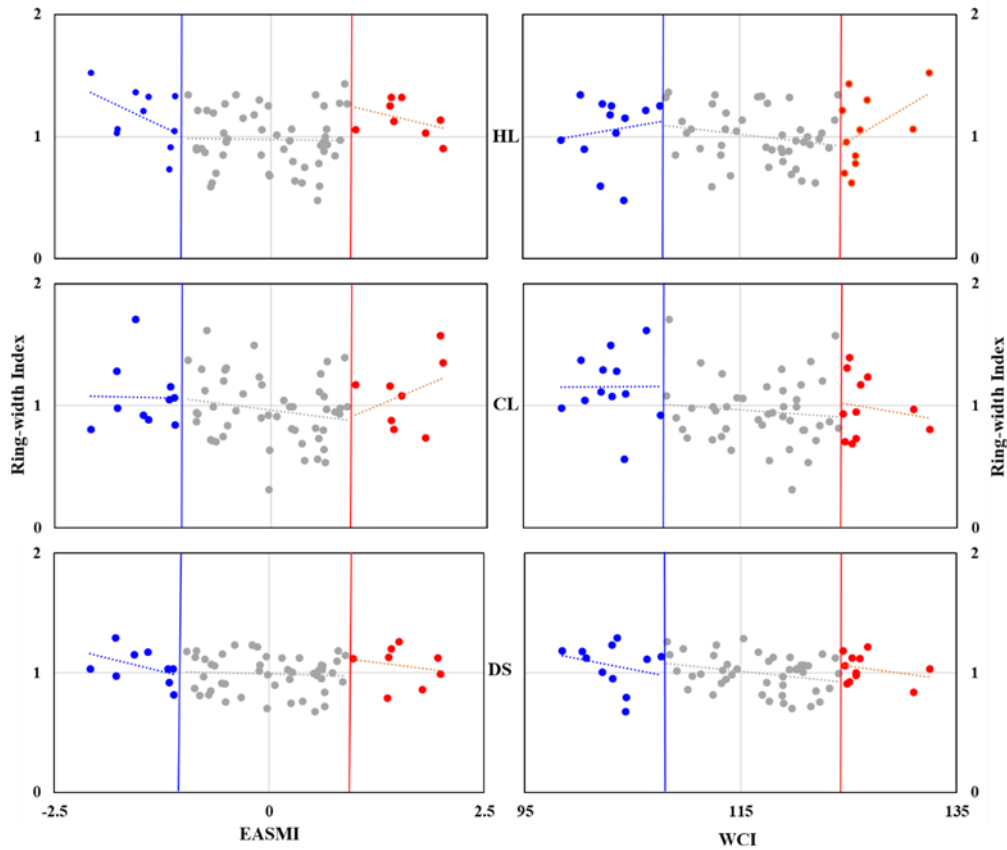
390 At CL, correlations between the higher and middle ring-width groups to the WCI
391 and the higher and middle WCI groups to the ring-width index were all negative.
392 Correlations between the higher and middle ring-width groups and the EASMI, and
393 between the higher and middle EASMI groups with the ring-width index were
394 inconsistent (Fig. 6; 7).

395 At DS, correlations between the higher and lower ring-width groups and the
 396 EASMI, and between the higher and lower EASMI groups to the ring-width indices,
 397 were consistent. The correlations between the higher ring-width groups and the WCI,
 398 and between the higher WCI groups and the ring-width index were consistent. However,
 399 the correlations between the lower ring-width groups and the WCI, also between the
 400 lower WCI groups and the ring-width index, were inconsistent (Fig. 6; 7).



401
 402 Figure 6. Grouping related charts among the ring-width index of three regions (HL,
 403 CL and DS) and the two atmospheric circulations' indices (EASMI and WCI), grouped
 404 by chronological values. The noted numbers are the person correlation coefficients
 405 (two-tails test) and the corresponding significant credible level. Only the significant
 406 correlations were labeled. Red dots indicate the higher ring-width index group (>
 407 mean+1δ), gray dots indicate the middle ring-width index group (> mean-1δ ~<
 408 mean+1δ), and blue dots indicate the lower ring-width index group (> mean-1δ).

409 Except for HL, none of the ring-width groups or the atmospheric circulation index
 410 groups of the others reached a level of significance. These results suggest that HL is
 411 strongly affected by size of, and the interaction between, the EASM and the Westerly
 412 winds. On an interannual scale, stronger west winds and a weaker monsoon could result
 413 in variations from the ordinary climate (veering towards drier or wetter). Weaker west
 414 winds and a stronger monsoon formed the normal climate at HL. At the CL and DS
 415 sites, both atmospheric circulations were relatively weak on interannual scales. They
 416 had complex interactions.



417

418 Figure 7. Grouping related charts among the two atmosphere circulations' index
 419 (EASMI and WCI) and the ring-width index of three regions (HL, CL, and DS),
 420 grouped by the two atmosphere circulations' index. Red dots indicate the higher
 421 atmosphere circulations' index group ($> \text{mean}+1\delta$), gray dots indicate the middle
 422 atmosphere circulations' index group ($> \text{mean}-1\delta \sim < \text{mean}+1\delta$), and blue dots indicate
 423 the lower atmosphere circulations' index group ($> \text{mean}-1\delta$).

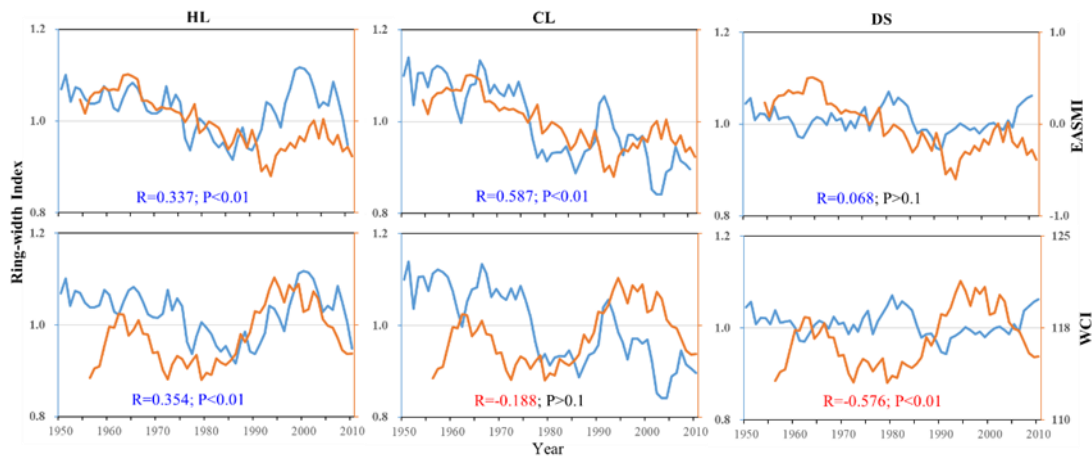
424

425 3.4.2 Driving mechanisms of the regional climate changes on a decadal scale

426 At HL, both the EASM and the westerly circulation had highly significant effects on
 427 the radial growth of the Qinghai spruce. At CL, the EASM also had highly significant
 428 effects on radial growth of the Qinghai spruce. There, correlation coefficients were
 429 higher for the EASMI (EASM index) than they were for the HL index. Correlations
 430 between the WCI and radial growth were negative, but not at a significant level.

431 At DS, correlation between radial growth and the WCI was extremely negative (P
 432 < 0.01). Correlation between radial growth and the EASM was positive ($P > 0.1$) (Fig.
 433 8). These results suggest that at HL, alternations between dry and wet seasons were

434 affected both by the EASM and the westerlies. If either of the two atmospheric
 435 circulations was stronger, the climate tended to be wetter. At CL, alternations between
 436 dry and wet were affected mainly by the EASM. When the EASM was stronger, the
 437 climate was wetter. At DS, the climate was affected mainly by the westerlies. The
 438 stronger the winds, the wetter the climate (Fig. 8).



439

440 Figure 8. Interdecadal scale (11-a running average) correlations of the three residual
 441 chronologies with the EASMI and WCI.

442 The results of our interdecadal partial correlation analysis of the three RES-
 443 chronologies with the WCI and EASMI further illustrate the impacts of the two
 444 circulation systems on the climate of the three regions (Table 2).

445 At HL, if we control one variable (the WCI or EASMI) from our analysis, the other
 446 variable will all showed a positive correlation with its chronology ($P < 0.0001$). At CL,
 447 if we controlled the WCI, we find a positive significant correction between the
 448 chronology and EASMI ($P < 0.0001$). If we controlled the effect of EASMI, we saw a
 449 weak negative correction between the chronology and WCI (Table 2). At DS, if we
 450 controlled EASMI, we saw a negative significant correlation between the chronology
 451 and WCI ($P < 0.0001$). If we controlled the WCI, we saw an insignificant negative
 452 correlation between the chronology and EASMI (Table 2).

453

454 Table 2. Inter-decadal partial correlation analysis of the three residual-chronologies
 455 with the WCI and EASMI.

	HL	CL	DS
WCI	0.489 ***	0.550***	-0.172
EASMI	0.511***	-0.001	-0.591***

456 Correlation significance levels (two-tailed test): *** P < 0.001.

457 Summary: at HL (on the eastern boundary of the Alxa Plateau), both EASMI and
 458 WCI influenced the alternation between wet and dry; at CL (on the southern boundary
 459 of the Alxa Plateau), climate was mainly influenced by the EASM. At DS (on the
 460 western boundary of the Alxa Plateau and the middle part of Hexi Corridor), climate
 461 was mainly influenced by the westerlies.

462

463 **4. Discussion and conclusions**

464 **4.1 Climate changes indicated by regional chronologies**

465 Our chronology-climate response analysis (Fig. 4) showed that the radial growth index
 466 of Qinghai spruce in the HL, CL and DS mountains were a good record of regional
 467 climate changes around the Alxa Plateau (Fig. 3). On the interannual scale, the three
 468 regional chronologies noted that the extreme drought years of 1928, 1957 and 1981
 469 were shared by two or more locations, as were the drought years of 1854, 1861, 1916,
 470 1926, 1947, 1966, and 2001 (Fig. 3).

471 We note that drought was also reported by other tree-ring studies for these regions
 472 (Chen et al., 2016), also for the Qilian Mountains (Zhang et al., 2011; Zhang et al.,
 473 2017). Several other drought years (1854, 1884, and 1925–1928) were also seen in the
 474 dry-wet climate history (PDSI and recorded by tree-ring-widths) in the nearby area of
 475 Mount Hasi, which lies on the edge of the regions most influenced by the EASM (Kang
 476 et al., 2012).

477 The drought years of 1823, 1833, 1854, 1877, 1883–1885, 1895, 1908, 1971, 1992,
 478 and 2003 seen in results for the Alxa Plateau are also seen in twelve tree-ring
 479 reconstructed drought series for the Qilian Mountains (an area mainly influenced by
 480 westerlies) (Zhang et al., 2011). We also note that wetter years seen in our three regional

481 chronologies were also seen in results from the Hasi and Xinglong Mountains, which
482 are also on the edge of the area influenced by the EASM) (Fang et al., 2009; Kang et
483 al., 2012).

484 If we compare our results with those seen for the EASM-affected areas at Mount
485 Guiqing, 1820–2005 (Fang et al., 2010), we noted that only three of the eight drought
486 years in that area (1928, 2000, and 2001) were seen in our three chronologies. We also
487 noted results from the westerly-influenced area at Mount Tianshan (Jiang et al., 2017).
488 The wetter years of 1846, 1903 and 1942 at DS were also extreme wet years at Mount
489 Tianshan. Two wet years, 1848 and 1959, recorded at DS are either one year earlier or
490 one year later than extremely wet years at Mount Tianshan, which might suggest some
491 correlation. Drier years at DS (1884, 1947 and 1951) are one or two years later than the
492 extremely dry years at Mount Tianshan. This suggests that these phenomena could be
493 related to broader changes in the extent and strength of the atmospheric circulation.

494 On a broader (interdecadal) scale, an extreme drought period in 1920s–1930s was
495 shared by much of northern China (Liang et al., 2006; Fang et al., 2009; Fang et al.,
496 2010). This is the same drought that we note our chronologies for HL, CL and DS (Liu
497 et al., 2002; Chen et al., 2010; Fan et al., 2012; Liu et al., 2013; Zhang et al., 2015). A
498 drought in 1890–1900 was noted by dendrochronological studies and regional history
499 documents (Yuan, 1994; Ma et al., 2003; Cai and Liu, 2007).

500 Ma and Fu's (2006) study showed a broad shift towards a drying climate in 1977–
501 78 (eastern area in northwestern China, also northern China). Several other
502 dendrochronological studies showed a combination of high temperatures and low
503 precipitation in the late 1970s to early 1990s (Zhang et al., 2005b; Cai and Liu, 2007;
504 Cai, 2009). This same drought was seen at DS, if somewhat later and for a shorter time.
505 We also noted its effects at HL and CL. This would be consistent with the increased
506 humidity of the climate in the eastern region of Northwest China (the EASM-influenced
507 region experiencing > 400 mm precipitation). This region would include Mount
508 Xinglong (Fang et al., 2009; Chen et al. 2015), the easternmost part of the Qilian
509 Mountains, and Mount Guiqing (Fang et al., 2010).

510 The wet period that lasted from the 1940s to the early 1970s has been recorded by
511 several tree-ring-width chronologies covering HL, CL, and DS (Liu et al., 2004; Liu et
512 al., 2005; Gao et al., 2006; Cai, 2009; Chen et al., 2010). Regional history documents
513 also record some severe floods disasters in this period (Yuan, 1994). We also see this
514 wet period in tree-ring-width chronologies from Mount Xinglong (Fang et al., 2009;
515 Chen et al. 2015) and Mount Guiqing (Fang et al., 2010).

516 The wet period in the 1830s–1840s evident in the chronologies in Xinglong
517 Mountain (Fang et al., 2009) (Chen et al. 2015) and Guiqing Mountain (Fang et al.,
518 2010) corresponds to the dry period of DS. The wet period in the 1830s–1840s
519 corresponds to the dry period of HL and CL, and to the wet period of DS. The observed
520 phenomena can be attributed to differences in the extent and intensity of EASM and
521 westerly atmospheric circulations.

522

523 **4.2 Influence of atmospheric circulations and their interaction on climate change** 524 **in the Alxa Plateau**

525 Water vapor carried by the westerlies will extend southward to the northern part of
526 Qinghai, the Hexi region of Gansu, the northern part of Ningxia, and the northern part
527 of Shaanxi Province, sometimes passing through the northern border of the Xinjiang
528 region (Li et al., 2012). The area bounded by 35° and 55°N, and 110°E and 140°E seems
529 to be crucial to fluctuations in the westerlies. This in turn affects the distribution of rain
530 belts in summer. Its mean WCI are weaker positively to the rainfall in the middle of
531 Yellow River Basin and its northern regions (Yan et al., 2007). The results showed that
532 the middle ring-width index group of Qinghai spruce in the three sample sites, which
533 are located in the key area for interaction between wind and monsoon, presented weaker
534 negative correlation with WCI on the interannual scale (Fig. 6).

535 The EASM boundary zone has a greater influence on precipitation at higher
536 latitudes and thus on vegetation growth. This boundary zone can fluctuate due to the
537 interannual variability of the EASM and the westerlies. There may be lagging effects
538 at the mid-latitudes (Ou and Qian, 2006). Again, we note that on an interannual scale,

539 there is much variation in the strengths and interactions of the EASM and westerly
540 circulation and thus on climate in our three study regions (Fig. 6).

541 Sun et al. (2019) showed that when the westerly circulation strengthens, high
542 latitude air pressure drops across the entire Asian continent. Siberian high pressures and
543 the EASM are weakened. The south of the cold air activity is also correspondingly
544 weakened. That is not conducive to the north and south of the cold and warm air vapor
545 exchange to form precipitation. When the lower of the WCI and weakened latitudinal
546 circulation, the meridional circulation will strengthen, which favors the exchange of
547 warm and cold air between the north and south to form precipitation.

548 Yang et al. (2019) proposed that in years with weak summer westerlies in the
549 middle latitudes, the upper-level jet stream tends to shift southward. This southward
550 displacement of the jet stream, coupled with weakened lower-level divergence, hampers
551 the northward transport of warm air into the southwestern region. Consequently, this
552 leads to reduced availability of water vapor sources and ultimately results in diminished
553 summer precipitation within the transitional zone of typical monsoon activity. If the jet
554 stream moves northward, precipitation increases.

555 Xu et al. (2010) wrote that in the middle Qilian Mountains the westerlies affect
556 precipitation directly, while the EASM only indirectly affects precipitation. When the
557 westerlies are stronger, the high precipitation zone moves northwestward; when they
558 are weaker, the zone moves southeastward.

559 At DS, radial growth showed weak negative correlations with higher WCI and also
560 higher, middle, and lower EASMI groups (Figs. 6; 7). At HL, when high chronology
561 indices are positive they are significantly correlated with westerly circulation; when
562 they are negative they significantly correlate with EASM (Figs. 6; 7). At CL, which lies
563 further to the south than HL, a higher EASMI leads to a more humid climate. Other
564 effects are more complicated: for example, the higher and lower ring-width index
565 groups, associated with extreme dry and wet climate years, have weak negative
566 correlations to EASMI (Figs. 6; 7). Jiang et al. (2019) published the results of their
567 hydrogen and oxygen isotope studies of surface water at more than 3,000 sampling sites
568 in northern China. They showed that surface water recharge in the DS Mountains is due

569 to the westerlies; recharge in the CL Mountains is due to the EASM. The HL Mountains,
570 in contrast, sit at the boundary of the EASM; water recharge there is due to both the
571 EASM and the westerlies.

572 Jiang and Wang (2005) notes significant declines in the EASM in the mid-1960s
573 and mid-1970s, which led to decline in the radial growth of Qinghai spruce in our study
574 area. The effect of the latter declined period was much greater than that of the former,
575 whatever the intensity or duration. The effects of these declines were stronger at CL
576 and DS than at HL. In the mid-1970s, EASM retreat had stronger negative effects at
577 CL and then at HL. However, decline in the EASM proved to be a facilitator of radial
578 growth at DS (Fig. 8).

579 In the same period the westerly circulation also retreated. The EASM retreated
580 again in 1990s, while the westerlies strengthened. This resulted in a drier climate in the
581 CL Mountains. However, it was also correlated with fluctuating wet periods at HL and
582 a weak wet period at DS. The above results, to a certain extent, support our view on the
583 driving mechanisms of climate change in the three study areas, especially in the DS
584 Mountains.

585 When we look at this area on a geologic scale, we learn that the westerly circulation
586 strengthened during the Ice Age. Westerly jet streams moved southward to about 35°N.
587 When the westerlies weakened in the Interglacial Age, the westerly jet streams moved
588 northward to ~37°N (Sun et al., 2003). A study of Holocene lake level evolution in the
589 ancient Zhuye lake, central Alxa Plateau, showed that lake-level change was subject to
590 the combined effects of EASM and the arid climate of Central Asia (Li, 2009) This
591 result further illustrates the complexity of lake evolution and climate change in the
592 EASM marginal zone.

593 The westerly circulation also interacts with the monsoon on the Tibetan Plateau,
594 which has a profound effect on the climate of the Asian monsoon region as well as the
595 global climate (Qu et al., 2004). There has also been much research using proxy
596 indicator cycles indicating that our study area is also influenced by large-scale climate
597 and ocean-atmosphere changes on interannual and interdecadal scales, such as the
598 North Atlantic Oscillation (NAO), Pacific Decadal Oscillation (PDO), El Niño-

599 Southern Oscillation (ENSO), and sunspot activity (Gou et al., 2015a; 2015b; Liu et al.,
600 2016; Wang et al., 2017).

601 However, all of the above-mentioned large-scale climate and ocean-atmosphere
602 changes affect the EASM and westerly circulation through different pathways (Li.
603 2009), which in turn have various effects on the northwestern edge zone of the EASM
604 and the zone of interaction between the two major atmospheric circulations.

605 In conclusion, based on the analysis of the regional chronologies collected in the
606 HL, CL and DS mountains that are arrayed around the Alxa Plateau, we can safely assert
607 that the radial growth of Qinghai spruce in the study area is mainly affected by regional
608 precipitation. This precipitation varies constantly over time and space, primarily
609 influenced by the interactions between two atmospheric circulation systems, EASM
610 and westerlies. At HL, both of these atmospheric circulation systems play a significant
611 role in shaping climate changes. At CL, the climate is mainly influenced by the EASM.
612 At DS, climate is more heavily influenced by the westerly circulation.

613 In the future, it is to be hoped that more refined, smaller scale research can be done
614 on the climate history in the deserts of the Alxa Plateau. Such research may finally to
615 provide a theoretical basis to explain regional climate driving mechanisms and thus
616 enable better desertification controls.

617

618 **Acknowledgements**

619 The study was jointly funded by the National Natural Science Foundation of China
620 (NSFC) (No.42171031; 42171167); Inner Mongolia Autonomous Region Special Fund
621 project for transformation of Scientific and technological Achievements (2021CG0046).

622

623 **References**

624 Cai, Q. F.: Response of *Pinus tabulaeformis* tree-ring growth to three moisture indices and
625 January to July Walter index reconstruction in Helan mountain, *Marine geology &*
626 *Quaternary geology*, 29, 131–136 (In Chinese with English abstract),
627 <https://doi.org/10.3724/SP.J.1140.2009.06131>, 2009.

628 Cai, Q. F. and Liu, Y.: January to August temperature variability since 1776 inferred from tree-
629 ring width of *Pinus tabulaeformis* in Helan Mountain, *Journal of Geographical Sciences*,

- 630 17, 293–303, <https://doi.org/10.1007/s11442-007-0293-5>, 2007.
- 631 Chen, F., Yuan, Y. J., Zhang, T. W., and Linderholm, H. W.: Annual precipitation variation for
632 the southern edge of the Gobi Desert (China) inferred from tree rings: linkages to climatic
633 warming of twentieth century, *Nat. Hazards*, 81, 939–955, [https://doi.org/10.1007/s11069-](https://doi.org/10.1007/s11069-015-2113-z)
634 015-2113-z, 2016.
- 635 Chen, F., Wei, W. S., Yuan, Y. J., Yu, S. L., Shang, H. M., Zhang, T. W., Zhang, R. B., Wang, H.
636 Q., and Qin, L.: Variation of annual precipitation during 1768-2006 in Gansu Inferred from
637 multi-site tree-ring chronologies, *Journal of Desert Research*, 33, 1520–1526 (In Chinese
638 with English abstract), <https://doi.org/10.7522/j.issn.1000-694X.2013.00218.>, 2013.
- 639 Chen, F., Yuan, Y. J., Wei, W. S., Yu, S. L., Fan, Z. A., Zhang, R. B., Zhang, T. W., Li, Q., and
640 Shang, H. M.: Temperature reconstruction from tree-ring maximum latewood density of
641 Qinghai spruce in middle Hexi Corridor, China, *Theoretical and Applied Climatology*, 107,
642 633–643, <https://doi.org/10.1007/s00704-011-0512-y>, 2012.
- 643 Chen, F., Yuan, Y. J., Wei, W. S., Yu, S. L., Li, Y., Zhang, R., Fan, Z., Zhang, T., and Shang, H.:
644 PDSI changes of May to July recorded by tree rings in the northern Helan Mountains,
645 *Advance in Climate Changes Research*, 65, 344-348 (In Chinese with English abstract),
646 2010.
- 647 Chen, F. H., Chen, J. H., Huang, W., Chen, S. Q., Huang, X. Z., Jin, L. Y., Jia, J., Zhang, X. J.,
648 An, C., and Zhang, J.: Westerlies Asia and monsoonal Asia: spatiotemporal differences in
649 climate change and possible mechanisms on decadal to sub-orbital timescales, *Earth-Sci.*
650 *Rev.*, 192, 337–354, <https://doi.org/10.1016/j.earscirev.2019.03.005>, 2019a.
- 651 Chen, F. H., Fu, B. J., Xia, J., Wu, D., Wu, S. H., Zhang, Y. L., Sun, H., Liu, Y., Fang, X. M.,
652 Qin, B. Q., Li, X., Zhang, T. J., Liu, B. Y., Dong, Z. B., Hou, S. G., Tian, L. D., Xu, B. Q.,
653 Dong, G. H., Zheng, J. Y., Yang, W., Wang, X., Li, Z. J., Wang, F., Hu, Z. B., Wang, J.,
654 Liu, J. B., Chen, J. H., Huang, W., Hou, J. Z., Cai, Q. F., Long, H., Jiang, M., Hu, Y. X.,
655 Feng, X. M., Mo, X. G., Yang, X. Y., Zhang, D. J., Wang, X. H., Yin, Y. H., and Liu, X.
656 C.: Major advances in studies of the physical geography and living environment of China
657 during the past 70 years and future prospects, *Science China Earth Sciences*, 62, 1665–
658 1701, <https://doi.org/10.1007/s11430-019-9522-7>, 2019b.
- 659 Chen, J., Huang, W., Jin, L., Chen, J. H., Chen, S. Q., and Chen, F. H.: A climatological northern
660 boundary index for the East Asian summer monsoon and its interannual variability,
661 *Science China Earth Sciences*, 61, 13–22, <https://doi.org/10.1007/s11430-017-9122-x>,
662 2018.
- 663 Cook E.R.: A Time Series Analysis approach to tree ring standardization (Dendrochronology,
664 forestry, dendroclimatology, autoregressive process)[D]. Tuscon, Arizona: The University
665 of Arizona, 1985.
- 666 Ding, Y. H., Liu, Y. J., Xu, Y., Wu, P., Xue, T., Wang, J., Shi, Y., Zhang, Y. X., Song, Y. F., and
667 Wang, P. L.: Regional responses to global climate change: progress and prospects for trend,
668 causes, and projection of climatic warming-wetting in Northwest China, *Advances in*
669 *Earth Science*, 38, 551–562 (In Chinese with English abstract),

- 670 <https://doi.org/10.11867/j.issn.1001-8166.2023.027>, 2023.
- 671 Fan, Z. A., Wei, W. S., Chen, F., and Yuan, Y. J.: Precipitation variation from 1775 to 2005 at
672 the eastern margin of Tengger Desert, China inferred from tree-ring, *Journal of Desert*
673 *Research*, 32, 996–1002 (In Chinese with English abstract), 2012.
- 674 Fang, K. Y., Gou, X. H., Chen, F. H., D'arrigo, R., and Li, J. B.: Tree-ring based drought
675 reconstruction for the Guiqing Mountain (China): linkages to the Indian and Pacific
676 Oceans, *Int. J. Climatol.*, 30, 1137–1145, <https://doi.org/10.1002/joc.1974>, 2010.
- 677 Fang, K. Y., Gou, X. H., Chen, F. H., Yang, M. X., Li, J. B., He, M. S., Zhang, Y., Tian, Q. H.,
678 and Peng, J. F.: Drought variations in the eastern part of northwest China over the past two
679 centuries: evidence from tree rings, *Clim. Res.*, 38, 129–135,
680 <https://doi.org/10.3354/cr00781>, 2009.
- 681 Feng, W., Wang, K. L., and Jiang, H.: Influences of westerly wind inter-annual change on water
682 vapor transport over northwest china summer, *Plateau Meteorology*, 23, 270–275 (In
683 Chinese with English abstract), 2004.
- 684 Gao, S. Y., Lu, R. J., Qiang, M. R., Ha, S., Zhang, D. S., Chen, Y., and Xia, H.: Precipitation
685 variation recorded by tree-rings in the northern Tengger Desert of the last 140 years, *Chin.*
686 *Sci. Bull.*, 51, 326–331, <https://doi.org/10.1360/csb2006-51-3-326>, 2006.
- 687 Gou, X. H., Gao, L. L., Deng, Y., Chen, F. H., Yang, M. X., and Still, C.: An 850 - year tree -
688 ring - based reconstruction of drought history in the western Qilian Mountains of
689 northwestern China, *Int. J. Climatol.*, 35, 3308–3319, <https://doi.org/10.1002/joc.4208>,
690 2015a.
- 691 Gou, X. H., Deng, Y., Gao, L. L., Chen, F. H., Cook, E., Yang, M. M., and Zhang, F.: Millennium
692 tree-ring reconstruction of drought variability in the eastern Qilian Mountains, northwest
693 China, *Climate Dynamics*, 45, 1761–1770, <https://doi.org/10.1007/s00382-014-2431-y>,
694 2015b.
- 695 Huang, L. X., Chen, J., Yang, K., Yang, Y. J., Huang, W., Zhang, X., and Chen, F. H.: The
696 northern boundary of the Asian summer monsoon and division of westerlies and monsoon
697 regimes over the Tibetan Plateau in present-day, *Science China Earth Sciences*, 66, 882–
698 893, <https://doi.org/10.1007/s11430-022-1086-1>, 2023.
- 699 Jiang, D. B. and Wang, H. J.: Natural interdecadal weakening of East Asian summer monsoon
700 in the late 20th century, *Chin. Sci. Bull.*, 50, 1923–1929, [https://doi.org/10.1360/982005-](https://doi.org/10.1360/982005-36)
701 36, 2005.
- 702 Jiang, P., Liu, H. Y., Wu, X. C., and Wang, H. Y.: Tree-ring-based SPEI reconstruction in central
703 Tianshan Mountains of China since A.D. 1820 and links to westerly circulation, *Int. J.*
704 *Climatol.*, 37, 2863–2872, <https://doi.org/10.1002/joc.4884>, 2017.
- 705 Jiang, W. J., Wang, G. C., Sheng, Y. Z., Shi, Z. M., and Zhang, H.: Isotopes in groundwater (^2H ,
706 ^{18}O , ^{14}C) revealed the climate and groundwater recharge in the Northern China, *Sci. Total*
707 *Environ.*, 666, 298–307, <https://doi.org/10.1016/j.scitotenv.2019.02.245>, 2019.

- 708 Kang, S. Y. and Yang, B.: Precipitation variability at the northern fringe of the Asian summer
709 monsoon in Northern China and its possible mechanism over the past 530 years,
710 Quaternary Sciences, 35, 1185–1193, <https://doi.org/10.11928/j.issn.1001-7410.2015.05.14>, 2015.
- 712 Kang, S. Y., Yang, B., and Qin, C.: Recent tree-growth reduction in north central China as a
713 combined result of a weakened monsoon and atmospheric oscillations, *Clim. Change*, 115,
714 519–536, <https://doi.org/10.1007/s10584-012-0440-6>, 2012.
- 715 Li, D. L., Shao, P. C., and Wang, H.: The position variations of the north boundary of East Asia
716 subtropical summer monsoon in 1951–2009, *Journal of Desert Research*, 33, 1511–1519
717 (In Chinese with English abstract), <https://doi.org/10.7522/j.issn.1000-694X.2013.00217>,
718 2013.
- 719 Li, J. L., Li, Z. R., Yang, J. C., Shi, Y. Z., and Fu, J.: Analyses on spatial distribution and
720 temporal variation of atmosphere water vapor over northwest China in summer of later 10
721 years, *Plateau Meteorology*, 31, 1574–1581 (In Chinese with English abstract), 2012.
- 722 Li, J. P. and Zeng, Q. C.: A new monsoon index, its interannual variability and related with
723 monsoon precipitation, *Climatic and Environmental Research*, 10, 351–365 (In Chinese
724 with English abstract), 2005.
- 725 Li, W. L., Wang, K. L., Fu, S. M., and Jiang, H.: The interrelationship between regional Westerly
726 index and the water vapor budget in Northwest China, *Journal of Glaciology and
727 Geocryology*, 30, 28–34 (In Chinese with English abstract), 2008.
- 728 Li, Y.: The pollen records from lake sediments and climate & lake model in the Marginal area
729 of Asian monsoon, Lanzhou University, Lanzhou, China, 2009.
- 730 Li, Z. X., Feng, Q., Song, Y., Wang, Q. J., Yang, J., Li, Y. G., Li, J. G., and Guo, X. Y.: Stable
731 isotope composition of precipitation in the south and north slopes of Wushaoling Mountain,
732 northwestern China, *Atmospheric Research*, 182, 87–101,
733 <https://doi.org/10.1016/j.atmosres.2016.07.023>, 2016.
- 734 Liang, E. Y., Liu, X. H., Yuan, Y. J., Qin, N. S., Fang, X. Q., Huang, L., Zhu, H. F., Wang, L.,
735 and Shao, X. M.: The 1920s drought recorded by tree rings and historical documents in
736 the semi-arid and arid areas of Northern China, *Clim. Change*, 79, 403–432,
737 <https://doi.org/10.1007/s10584-006-9082-x>, 2006.
- 738 Liu, J. B., Chen, J., Chen, S. Q., Yan, X. W., Dong, H. R., and Chen, F. H.: Dust storms in
739 northern China and their significance for the concept of the Anthropocene, *Science China
740 Earth Sciences*, 65, 921–933, <https://doi.org/10.1007/s11430-021-9889-8>, 2022.
- 741 Liu, Y., Cai, Q. F., Ma, L. M., and An, Z. S.: Tree ring precipitation records from Baotou and
742 the East Asia summer monsoon variations for the last 254 years, *Earth Sci. Front.*, 8, 91–
743 97 (In Chinese with English abstract), <https://doi.org/10.3321/j.issn:1005-2321.2001.01.012>, 2001.
- 745 Liu, Y., Sun, C. F., Li, Q., and Cai, Q. F.: A *Picea crassifolia* tree-ring width-based temperature
746 reconstruction for the Mt. Dongda region, Northwest China, and its relationship to large-

- 747 scale climate forcing, PLoS One, 11, e0160963,
748 <https://doi.org/10.1371/journal.pone.0160963>, 2016.
- 749 Liu, Y., Lei, Y., Sun, B., Song, H. M., and Li, Q.: Annual precipitation variability inferred from
750 tree-ring width chronologies in the Changling–Shoulu region, China, during AD 1853–
751 2007, *Dendrochronologia*, 31, 290–296, <https://doi.org/10.1016/j.dendro.2013.02.001>,
752 2013.
- 753 Liu, Y., Won-Kyu, P., Cai, Q. F., Jung-Wook, S., and Hyun-Sook, J.: Monsoonal precipitation
754 variation in the East Asia since A.D. 1840—tree-ring evidences from China and Korea,
755 *Science in China Series D: Earth Sciences*, 46, 1031–1039,
756 <https://doi.org/10.1007/BF02959398>, 2003.
- 757 Liu, Y., Ma, L. M., Cai, Q. F., An, Z. S., Liu, W. G., and Gao, L. Y.: Reconstruction of summer
758 temperature (June–August) at Mt. Helan, China, from tree-ring stable carbon isotope
759 values since AD 1890, *Science in China Series D: Earth Sciences*, 45, 1127–1136,
760 <https://doi.org/10.1360/02yd9109>, 2002.
- 761 Liu, Y., Cai, Q. F., Liu, W. G., Yang, Y. K., Sun, J. Y., Song, H. M., and Li, X. X.: Monsoon
762 precipitation variation recorded by tree-ring $\delta^{18}\text{O}$ in arid Northwest China since AD 1878,
763 *Chemical Geology*, 252, 56–61, <https://doi.org/10.1016/j.chemgeo.2008.01.024>, 2008.
- 764 Liu, Y., Cai, Q. F., Shi, J. F., Hughes, M. K., Kutzbach, J. E., Liu, Z. Y., Ni, F. B., and An, Z. S.:
765 Seasonal precipitation in the south-central Helan Mountain region, China, reconstructed
766 from tree-ring width for the past 224 years, *Canadian Journal of Forest Research*, 35,
767 2403–2412, <https://doi.org/10.1139/x05-168>, 2005.
- 768 Liu, Y., Shi, J. F., Shishov, V., Vaganov, E., Yang, Y. K., Cai, Q. F., Sun, J. Y., Wang, L., and
769 Djanseitov, I.: Reconstruction of May–July precipitation in the north Helan Mountain,
770 Inner Mongolia since A.D. 1726 from tree-ring late-wood widths, *Chin. Sci. Bull.*, 49,
771 405–409, <https://doi.org/10.1007/BF02900325>, 2004.
- 772 Ma, L. M., Liu, Y., Cai, Q. F., and An, Z. S.: The precipitation records from tree-ring late wood
773 width in the helan mountain, *Marine geology & Quaternary geology*, 23, 109–114 (In
774 Chinese with English abstract), <https://doi.org/10.16562/j.cnki.0256-1492.2003.04.016>,
775 2003.
- 776 Ma, M. J., Pu, Z. X., Wang, S. G., and Zhang, Q. A.: Characteristics and numerical simulations
777 of extremely large atmospheric boundary-layer heights over an arid region in north-west
778 china, *Boundary-Layer Meteorology*, 140, 163–176, <https://doi.org/10.1007/s10546-011-9608-2>, 2011.
- 780 Ma, Z. G. and Fu, C. B.: The basic facts of aridity in northern China from 1951 to 2004, *Chin.*
781 *Sci. Bull.*, 51, 2429–2439 (In Chinese), <https://doi.org/10.1360/csb2006-51-20-2429>,
782 2006.
- 783 Ou, T. H. and Qian, W. H.: Vegetation variations along the monsoon boundary zone in East
784 Asia, *Chinese Journal of Geophysics*, 49, 698–705 (In Chinese with English abstract),
785 2006.

- 786 Qin, L., Liu, G. X., Li, X. Z., Chongyi, E., Li, J., Wu, C. R., Guan, X., and Wang, Y.: A 1000-
787 year hydroclimate record from the Asian summer monsoon-Westerlies transition zone in
788 the northeastern Qinghai-Tibetan Plateau, *Clim. Change*, 176, 1–20, <https://doi.org/10.1007/s10584-023-03497-1>, 2023.
- 790 Qu, W. J., Zhang, X. H., Wang, D., Shen, Z. X., Mei, F. M., Cheng, Y., and Yan, L. W.: The
791 important significance of westerly wind study, *Marine Geology and Quaternary Geology*,
792 24, 125–132 (In Chinese with English abstract), <https://doi.org/10.16562/j.cnki.0256-1492.2004.01.018>, 2004.
- 794 Shao, X. M., Xu, Y., Yin, Z. Y., Liang, E. Y., Zhu, H. F., and Wang, S.: Climatic implications of
795 a 3585-year tree-ring width chronology from the northeastern Qinghai-Tibetan Plateau,
796 *Quaternary Science Reviews*, 29, 2111–2122,
797 <https://doi.org/10.1016/j.quascirev.2010.05.005>, 2010.
- 798 Sun, D. H., An, Z. S., Su, R. H., Deer, H. Y., and Sun, Y. B.: The dust deposition records of the
799 evaluation of Asia monsoon and Westerly circulation in north China in the last 2.6Ma,
800 *Science in China (Series D)*, 33, 497–504 (In Chinese), 2003.
- 801 Sun, L. Q., Li, T. J., Li, Q. L., and Wu, Y. P.: Responses of autumn flood peak in the Yellow
802 River source regions to westerly circulation index, *Journal of Glaciology and Geocryology*,
803 41, 1475–1482 (In Chinese with English abstract), <https://doi.org/10.7522/j.issn.1000-0240.2019.0028>, 2019.
- 805 Tang, X., Qian, W. H., and Liang, P.: Climatic features of boundary belt for East Asian Summer
806 Monsoon, *Plateau Meteorology*, 25, 375–381 (In Chinese with English abstract), 2006.
- 807 Vicente-Serrano, S.M., Beguería, S. and López-Moreno, J.I.: A multiscalar drought index
808 sensitive to global warming: the standardized precipitation evapotranspiration index. *J.*
809 *Clim.*, 23(7): 1696–1718, <https://doi.org/10.1175/2009jcli2909.1>, 2010.
- 810 Wang, B. J., Huang, Y. X., He, J. H., and Wang, L. J.: Relation between vapour transportation
811 in the period of East Asian Summer Monsoon and drought in Northwest China. *Plateau*
812 *Meteorology*, 23, 912–917 (In Chinese with English abstract), 2004.
- 813 Wang, J. L., Yang, B., Ljungqvist, F. C., Luterbacher, J., Osborn, Timothy j., Briffa, K. R., and
814 Zorita, E.: Internal and external forcing of multidecadal Atlantic climate variability over
815 the past 1,200 years, *Nature Geoscience*, 10, 512–517, <https://doi.org/10.1038/ngeo2962>,
816 2017.
- 817 Wang, K. L., Jiang, H., and Zhao, H. Y.: Atmospheric water vapor transport from westerly and
818 monsoon over the Northwest China, *Advances in Water Science*, 16, 432–438 (In Chinese
819 with English abstract), <https://doi.org/10.14042/j.cnki.32.1309.2005.03.021>, 2005.
- 820 Wigley, T.M.L., Briffa, K.R., Jones, P.D. On the average value of correlated time series, with
821 applications in dendroclimatology and hydrometeorology. *Journal of Climate and Applied*
822 *Meteorology* 23(2), 201–213, 1984.
- 823 Xiao, S. C., Chen, X. H., and Ding, A. J.: Study process of climate changes, environment
824 evolution and its driving mechanism in the last two centuries in the Alxa Desert, *Journal*

- 825 of Desert Research, 37, 1102–1201 (In Chinese with English abstract),
826 10.7522/j.issn.1000-694x.2017.00002, 2017.
- 827 Xiao, S. C., Yan, C. Z., Tian, Y. Z., Si, J. H., Ding, A. J., Chen, X. H., Han, C., and Teng, Z. Y.:
828 Regionalization for desertification control and countermeasures in the Alxa Plateau, China,
829 Journal of Desert Research, 39, 182–192 (In Chinese with English abstract),
830 <https://doi.org/10.7522/j.issn.1000-694X.2019.00068>, 2019.
- 831 Xu, J. J., Wang, K. L., Jiang, H., Li, Z. G., Sun, J., Luo, X. P., and Zhu, Q. L.: A numerical
832 simulation of the effects of Westerly and Monsoon on precipitation in the Heihe River
833 Basin, Journal of Glaciology and Geocryology, 32, 489–496 (In Chinese with English
834 abstract), 2010.
- 835 Yan, H. S., Hu, J., Fan, K., and Zhang, Y. J.: The analysis of relationship between the variations
836 of Westerly Index in summer and precipitation during the flood period over China in the
837 last 50 years. , Chinese Journal of Atmospheric Science, 31, 717–726 (In Chinese with
838 English abstract), 2007.
- 839 Yang, B., Qin, C., Wang, J. L., He, M. H., Melvin, T. M., Osborn, T. J., and Briffa, K. R.: A
840 3,500-year tree-ring record of annual precipitation on the northeastern Tibetan Plateau,
841 Proc. Natl. Acad. Sci. USA, 111, 2903–2908, <https://doi.org/10.1073/pnas.1319238111>,
842 2014.
- 843 Yang, J. H., Zhang, Q., Liu, X. Y., Yue, P., Shang, J. L., Ling, H., and Li, W. J.: Spatial-temporal
844 characteristics and causes of summer precipitation anomalies in the transitional zone of
845 typical summer monsoon, China, Chinese Journal of Geophysics, 62, 4120–4128 (In
846 Chinese with English abstract), <https://doi.org/10.6038/cjg2019M0639>, 2019.
- 847 Yuan, L.: Hazards history in northwestern China, Gansu people's press, Lanzhou, China1994.
- 848 Zhang, F., Chen, Q. M., Su, J. J., Deng, Y., Gao, L. L., and Gou, X. H.: Tree-ring recorded of
849 the drought variability in the northwest monsoon marginal, China, Journal of Glaciology
850 and Geocryology, 39, 245–251 (In Chinese with English abstract),
851 <https://doi.org/10.7522/j.issn.1000-0240.2017.0028>, 2017.
- 852 Zhang, Q., Yang, J. H., Wang, P. L., Yu, H. P., Yue, P., Liu, X. Y., Lin, J. J., Duan, X. Y., Zhu,
853 B., and Yan, X. Y.: Progress and prospect on climate warming and humidification in
854 Northwest China, Chin. Sci. Bull., 68, 1814–1828, <https://doi.org/10.1360/TB-2022-0643>,
855 2023.
- 856 Zhang, Q. B., Cheng, G. D., Yao, T. D., Kang, X. C., and Huang, J. G.: A 2,326 year tree-ring
857 record of climate variability on the northeastern Qinghai-Tibetan Plateau, Geophys. Res.
858 Lett., 30, 1739, <https://doi.org/10.1029/2003GL017425>, 2003.
- 859 Zhang, Q. L., Liu, W. G., Liu, Y., Ning, Y. F., and Wen, Q. B.: Relationship between the stable
860 carbon and oxygen isotopic compositions of tree ring in the Mt. Helan region,
861 Northwestern China, Geochimica, 34, 51–56, <https://doi.org/10.19700/j.0379-1726.2005.01.006>, 2005a.
- 863 Zhang, S., Xu, H., Lan, J. H., Goldsmith, Y., Torfstein, A., Zhang, G. L., Zhang, J., Song, Y. P.,

- 864 Zhou, K. E., Tan, L. C., Xu, S., Xu, X. M., and Enzel, Y.: Dust storms in northern China
865 during the last 500 years, *Science China Earth Sciences*, 64, 813–824,
866 <https://doi.org/10.1007/s11430-020-9730-2>, 2021.
- 867 Zhang, Y., Shao, X. M., Yin, Z. Y., Liang, E. Y., Tian, Q. H., and Xu, Y.: Characteristics of
868 extreme droughts inferred from tree-ring data in the Qilian Mountains, 1700-2005, *Clim.*
869 *Res.*, 50, 141–159, <https://doi.org/10.3354/cr01051>, 2011.
- 870 Zhang, Y. X., Yu, L., and Yin, H.: Annual precipitation reconstruction over last 191 years at the
871 south edge of Badain Jaran Desert based on tree ring width data, *Desert and Oasis*
872 *Meteorology*, 9, 12–16 (In Chinese with English abstract),
873 <https://doi.org/10.3969/j.issn.1002-0799.2015.01.003>, 2015.
- 874 Zhang, Y. X., Gou, X. H., Hu, W. D., Peng, J. F., and Liu, P. X.: The drought events recorded
875 in tree ring width in Helan Mt. over past 100 years, *Acta Ecologica Sinica*, 25, 2121–2126
876 (In Chinese with English abstract), 2005b.
877